(9) Greco, R.; Taylor, C. R.; Kramer, O.; Ferry, J. D. *J. Polym. Sci., Polym. Phys. Ed.* **1975**, *13*, 1687.
(10) Nelb, G. W.; Pedersen, S.; Taylor, C. R.; Ferry, J. D. *J. Polym. Sci., Polym. Phys. Ed.* **1980**, *18*, 645.
(11) Granick, S.; Pedersen, S.; Nelb, G. W.; Ferry, J. D.; Macosko, C. W. *J. Polym. Sci., Polym. Phys. Ed.* **1981**, *19*, 1745.
(12) Kan, H. C.; Ferry, J. D.; Fetters, L. J. *Macromolecules* **1980**, *13*, 1571.
(13) Kraus, G.; Rollmann, K. W. *J. Polym. Sci., Polym. Phys. Ed.* **1977**, *15*, 385.
(14) de Gennes, P. G. *Macromolecules* **1986**, *19*, 1245.
(15) Nielsen, L. E. *Mechanical Properties of Polymers and Composites*; Marcel Dekker: New York, 1975.
(16) Rouse, P. E. *J. Chem. Phys.* **1953**, *21*, 1272.
(17) Nemoto, N.; Moriwaki, M.; Odani, H.; Kurata, M. *Macromolecules* **1971**, *4*, 215.
(18) Nemoto, N.; Odani, H.; Kurata, M. *Macromolecules* **1972**, *5*, 531.
(19) Gotro, J. T.; Graessley, W. W. *Macromolecules* **1984**, *17*, 2767.
(20) Adachi, K.; Kotaka, T. *Macromolecules* **1985**, *18*, 466.

Solution-Cross-Linked Networks. 3. Dielectric Normal Mode Process of Guest Polyisoprene in Natural Rubber Networks

Beng Teik Poh,† Keiichiro Adachi,* and Tadao Kotaka

Department of Macromolecular Science, Faculty of Science, Osaka University, Toyonaka, Osaka 560, Japan. *Received February 6, 1987*

ABSTRACT: The "normal-mode process" of dielectric relaxation due to fluctuation of the end-to-end polarization vector was investigated on *cis*-polyisoprene (*cis*-PI) absorbed in cross-linked natural rubbers (NR) and a synthetic isoprene rubber (IR). When the network has the molecular weight between cross-links M_x higher than the molecular weight between entanglements M_e the dielectric relaxation times τ_{ng} of the guest *cis*-PI were ca. 0.4 decade higher than those in pure *cis*-PI. In terms of the tube theory of polymer dynamics, this enhancement of τ_{ng} of the guest molecules with molecular weight $M > M_e$ in the networks with $M_x \geq M_e$ was explained by the absence of the tube renewal effect in the networks. On the other hand, the τ_{ng}s of the guest molecules (with $M > M_e$) in the networks with $M_x < M_e$ were much longer than those in the pure state due to the "strangulation" effect as pointed out by de Gennes. The τ_{ng} in the strangulation state increased with M of the guest *cis*-PI with the power of 4.0 ± 0.5. The mean-square end-to-end distance $\langle r^2 \rangle$ of the guest *cis*-PI in the networks was calculated from the contribution of the guest *cis*-PI to the dielectric relaxation strength for the normal-mode process. In NR networks, the $\langle r^2 \rangle$s of the guest *cis*-PI were slightly smaller than the value $\langle r^2 \rangle_0$ in the unperturbed state presumably due to repulsive interactions caused by the difference in the microstructure between the *cis*-PI molecules and the NR networks, while that in the IR network was the same as $\langle r^2 \rangle_0$.

Introduction

In the first paper of this series,[1] we reported the swelling and absorption behavior of solution-cross-linked natural rubber (NR) toward benzene solutions of guest *cis*-polyisoprene (*cis*-PI). It was found that since the solution-cross-linked NRs have higher free energy than bulk-cross-linked networks, they exhibit high swellability toward polymers. Using this property, we studied the contribution of the guest *cis*-PI molecules entrapped in the NR networks to their viscoelastic properties and reported the results in part 2 of this series.[2] Particularly in the latter,[2] we demonstrated that the networks containing guest molecules are an interesting model system for investigating the dynamic behavior of entrapped polymer chains.

For the dynamics of polymer chains entrapped in a network, de Gennes[3] proposed a "phase diagram" (see Figure 1 of the part 2 of this series) that classifies schematically the behavior into three regions depending on the molecular weight M of the guest polymer (which we assume to be chemically identical with that of the network polymer), that between cross-links M_x, and that between entanglements M_e:[4] In the region where $M < M_e < M_x$, the free-draining Rouse model[5] prevails; in the region where $M_e < M$ and M_x, the reptation modes of the tube model[6,7] are dominant; in the region of $M > M_e > M_x$ called the "strangulation"[3] region, the entrapped guest molecules suffer from stronger confinement due to the network rather than that due to entanglement.

Although viscoelastic spectroscopy of the network/guest polymer systems provided interesting information on the dynamics of the entrapped guest molecules, the method has two difficulties: In the first place, to extract the contribution of the guest molecules, we need to employ an adequate rule of mixtures,[8] and second, such a contribution is often obscured by the network especially when the amount of entrapped guest chains is small.

Previously, we demonstrated that *cis*-PI has a component of the dipole moment aligned parallel along the chain contour, exhibiting the "dielectric normal mode" process arising from fluctuation of such an end-to-end polarization vector.[9,10] Thus, we can determine from this study not only the dynamic behavior including the relaxation times and their distribution, but also the conformational characteristics, particularly the mean-square end-to-end distance $\langle r^2 \rangle$ of *cis*-PI in solutions of infinite dilution to the bulk state.[11]

Obviously, the "dielectric normal-mode" spectroscopy is applicable to the network/guest *cis*-PI systems as well. Moreover, this method has an additional advantage that the contribution of guest *cis*-PI is easily extracted since closed loops of network strands in the natural rubber network should not, in principle, exhibit the dielectric normal-mode process.

In this study, taking the advantages of the dielectric method over the mechanical spectroscopy, we attempted to clarify the dynamic and conformational properties of

† Present address: School of Industrial Technology, Universiti Sains Malaysia, Minden, Penang, Malaysia.

0024-9297/87/2220-2574$01.50/0

Table I
Cross-Linking Concentration C_x (in Volume Fraction) and Molecular Weight between Cross-Links M_x[a]

code	C_x	$10^{-3}M_{xs}$	$10^{-3}M_{xE}$
NR(0.1:20)	0.11		3.0
NR(0.4:40)	0.42	6.0	4.5
NR(0.4:30)	0.42	7.2	3.3
NR(0.4:20)	0.42	8.1	3.8
NR(0.4:10)	0.42	9.7	3.4
NR(1:40)	1	3.0	1.3
NR(1:20)	1	2.9	1.1

[a] Subscripts s and E represent that M_x was determined from swelling ratio and Young's modulus, respectively.

guest *cis*-PI molecules in the networks of natural rubber (NR) samples and a synthetic isoprene rubber (IR) sample.

Theory

The complex dielectric constant $\epsilon^*(\omega)$ for the normal-mode process is written as

$$\frac{\epsilon^*(\omega) - \epsilon_\infty}{\Delta\epsilon} = \langle r^2\rangle^{-1} \int_0^\infty \frac{-\mathrm{d}}{\mathrm{d}t}\langle \mathbf{r}(0)\cdot\mathbf{r}(t)\rangle \exp(-i\omega t)\, \mathrm{d}t \quad (1)$$

$$\frac{\Delta\epsilon}{C} = \frac{4\pi N_A \mu^2 \langle r^2\rangle}{3k_B TM} \quad (2)$$

where ϵ_∞ is the unrelaxed dielectric constant; $\Delta\epsilon$, the dielectric relaxation strength; $\langle \mathbf{r}(0)\cdot\mathbf{r}(t)\rangle$, the autocorrelation function of the end-to-end vector $\mathbf{r}$; t, the time; ω, the angular frequency; C, the concentration of polymer (in wt/vol); and μ, the dipole moment per unit contour length. Strictly speaking, eq 1 should include the correlation function of $\mathbf{r}$ between different polymer molecules i and j. However, as far as *cis*-PI is concerned, $\langle \mathbf{r}_i(0)\cdot\mathbf{r}_j(t)\rangle$ is negligible.[12] We also assumed in eq 2 that the ratio of internal to external fields is unity.[13]

When uncross-linked polymers have molecular weight M smaller than the characteristic molecular weight M_c ($=2M_e$), $\langle \mathbf{r}(0)\cdot\mathbf{r}(t)\rangle$ is described by the Rouse theory.[11] According to Zimm,[14] the longest dielectric relaxation time $\tau_R(M)$ is just twice the mechanical longest relaxation time and is given by

$$\tau_R(M) = \zeta M\langle r^2\rangle/(3\pi^2 k_B TM_0) \quad (3)$$

where M_0 is the molecular weight of the monomer unit and ζ is the monomeric friction coefficient. On the other hand, the relaxation time for a chain having M greater than M_e is given by the relaxation time τ_d of the tube disengagement process in the tube theory:[7]

$$\tau_d = (M/M_e)\tau_R(M) \quad (4)$$

For the strangulation state where $M_x < M_e$, M_e in eq 4 can be replaced by M_x. Thus, the τ_d is given by

$$\tau_d = (M/M_x)\tau_R(M) \quad (5)$$

Experimental Section

Solutions of natural rubber with concentration C_x were cross-linked by ^{60}Co γ-rays. Samples of guest *cis*-PI were prepared by anionic polymerization.[9,10] The code of the network samples is NR(C_x in volume fraction:total dose of γ-rays in Mrd), and that of *cis*-PI is PI-weight-average molecular weight M divided by 1000. Details of the sample preparation and characterization were described in parts 1 and 2 of this series.[1,2] Synthetic *cis*-PI with $M = 7 \times 10^5$ having the same microstructure as the guest *cis*-PI was also cross-linked by γ-ray. This network was coded as IR-(C_x:dose). We determined M_x by two methods: M_{xE} and M_{xs} stand for the values of M_x determined from Young's modulus and the swelling ratio, respectively. The characteristics of the networks and the guest *cis*-PIs are listed in Tables I and II, respectively.

Table II
Characteristics of *cis*-Polyisoprene

code	$10^{-3}M_w$	$10^{-3}M_n$	M_w/M_n
PI-01		1.4	
PI-02		2.4	
PI-05		4.5	
PI-09	8.6		1.29
PI-11	11.0		1.17
PI-13	13.0		1.08
PI-14	14.4		1.05
PI-25	24.5		1.05
PI-31	31.2		1.09
PI-42	41.6		1.35

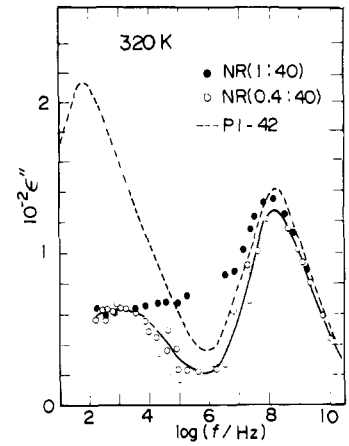

Figure 1. Frequency dependence of ϵ'' at 320 K for NR(1:40), NR(0.4:40), and PI-42.

Results and Discussion

Dielectric Relaxation of Network. Assuming the time–temperature superposition principle,[4] we constructed the master curves of the frequency f dependence of dielectric loss factor ϵ''. Figure 1 shows the ϵ'' curves reduced to T_r = 320 K for NR(0.4:40), NR(1:40), and PI-42.

As reported previously, uncross-linked *cis*-PI shows two distinct ϵ'' maxima (see the ϵ'' curve for PI-42 in Figure 1).[9,10] The high-frequency maximum is due to the segmental mode process and locates at about 10^8 Hz at 320 K independent of M. The low-frequency peak is due to the normal mode process and is quite sensitive to M. The loss maximum frequency f_{mn} decreases with increasing M.

Comparing the ϵ'' curves between the networks and PI-42, we see that the relaxation frequency and intensity of the segmental mode process are not affected by cross-linking. On the other hand, the shape of the ϵ'' curve in the range below 10^6 Hz is different from one sample to another. The networks show a broad ϵ'' peak having an intensity of $^1/_3$–$^1/_4$ of that of PI-42 in this loss frequency range. Two possibilities are raised as the origin of this loss maximum: One is some mobile chains included in the network and the other is the stretching motion of the network chains. However, it is expected that the contribution of the latter is much smaller than that of the former since usually the cross-link points are considered to be almost fixed.

Since the sol fraction had been thoroughly extracted after preparation of the networks, these broad loss maxima cannot be assigned to uncross-linked chains remaining in the networks. It appears that the small loss peak for NR(0.4:40) is due to the motion of dangling chains produced during the cross-linking reaction. We recognize that NR(1:40) shows the normal mode relaxation in a higher frequency range than NR(0.4:40). This suggests that the dangling chains in NR(1:40) are shorter than those in

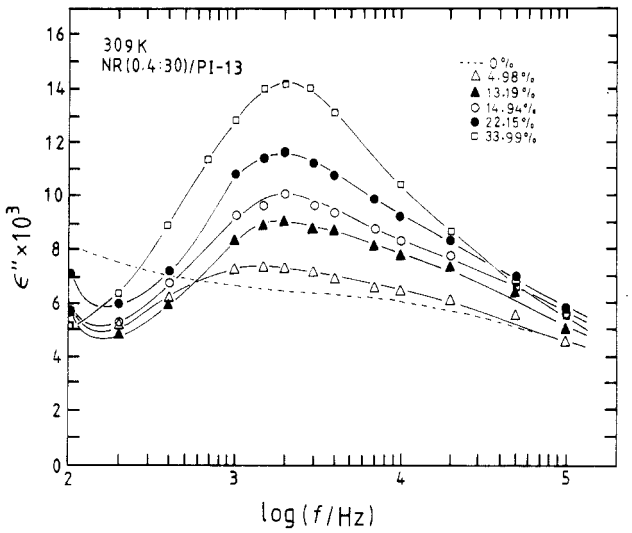

Figure 2. Frequency dependence of ϵ'' for the NR(0.4:30)/PI-13 system at 309 K.

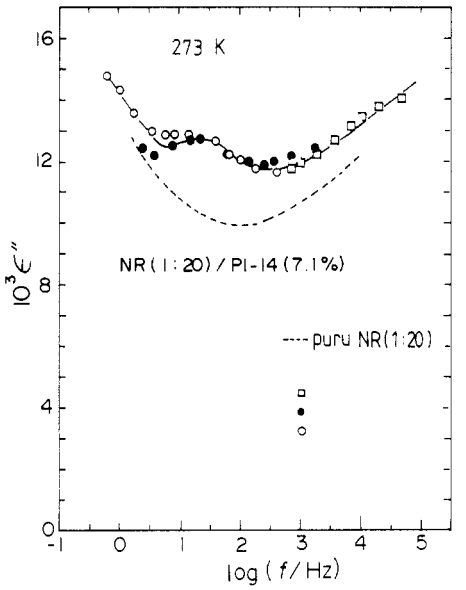

Figure 3. Frequency dependence of ϵ'' for the NR(1:20)/PI-14 system. Content of the guest *cis*-PI is 7.1 wt %. Dashed line indicates the ϵ'' curve for NR(1:20).

NR(0.4:40), since the cross-link density of NR(1:40) is higher than that of NR(0.4:40). Broadness of the loss curve can be attributed to the distribution of molecular weight of the dangling chains.

As mentioned above, the intensity of the loss is ca. $^1/_3$ of that of pure *cis*-PI. This indicates that the content of the dangling chain in the network is ca. $^1/_3$. Recently, Shy and Eichinger[15] made a computer calculation of the structure of networks prepared by irradiation cross-linking. If the ratio of the probabilities for cross-linking and chain scission is assumed to be 5, the content of the dangling chain becomes about 0.3 for the cross-link density of ca. 0.5%.[15] The present results agree with their calculation in order.

Network/Guest System. Figures 2–5 show the representative ϵ'' curves for the networks including the guest *cis*-PI. A clear ϵ'' peak is seen in the audiofrequency range of each curve. As seen in these figures, the loss maximum frequency f_{mn} increased with decreasing M as observed in uncross-linked *cis*-PI.[9,10] The amplitude of the loss peak increased with increasing content of the guest molecules. Therefore, these loss peaks can be assigned to the normal mode process of the guest *cis*-PI in the networks.

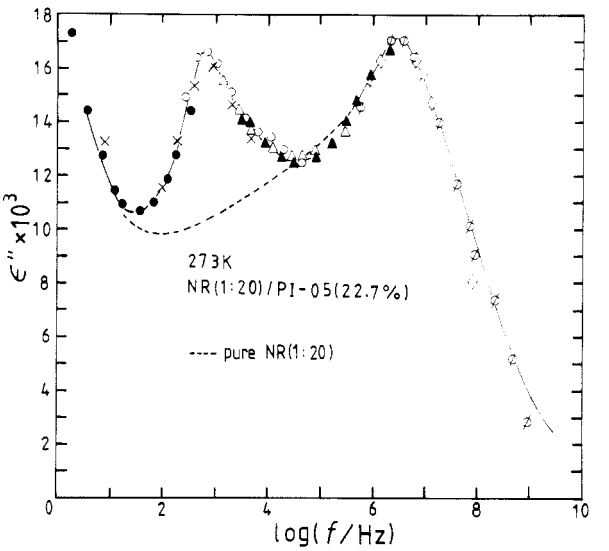

Figure 4. Frequency dependence of ϵ'' for the NR(1:20)/PI-05 system. Content of the guest is 22.7 wt %. Dashed line indicates the ϵ'' curve for NR(1:20).

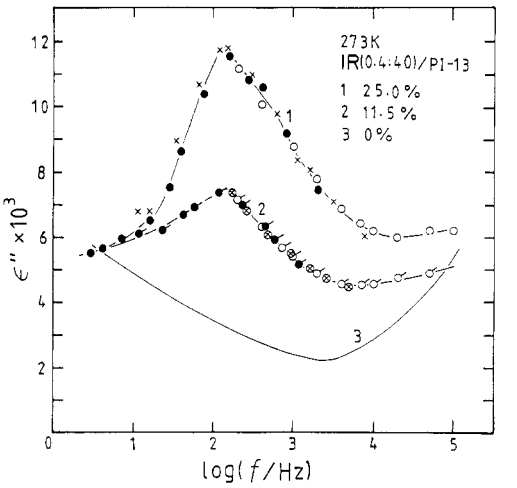

Figure 5. Frequency dependence of ϵ'' for IR(0.4:40) containing 11.5 and 25% PI-13.

We note that the loss maxima due to the guest *cis*-PI are much clearer than those observed in the mechanical loss curves reported in part 2 of this series.[2] Especially, for the low molecular weight *cis*-PI, we could not resolve the loss due to the guest molecules by viscoelastic spectroscopy because it overlapped with the dominant wedge-type loss curve of the network. In the ϵ'' curves, no wedge-type spectrum is observed. This is because the higher order modes of the Rouse theory[5] contribute equivalently to the mechanical relaxation, while the contribution of the pth normal mode to the dielectric relaxation is p^{-2}. A detailed comparison between the dielectric and mechanical relaxation spectra will be given elsewhere.

Shift Factor and Friction Coefficient. To compare the relaxation time of the guest *cis*-PI in the networks, it is necessary to separate the contribution of the local friction and the effect of entanglement. Generally, the relaxation times for large-scale motions such as those involved in the normal mode process are written in the form:[4,16]

$$\tau = \zeta f(M) \tag{6}$$

where ζ is the monomeric friction coefficient and $f(M)$ is the structural factor which depends on the architecture and molecular weight of the polymer but does not depend on its chemical structure and temperature. To discuss the

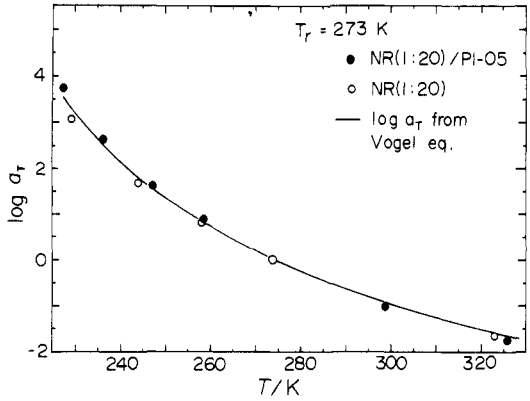

Figure 6. Shift factor a_T for pure NR(1:20) (○) and NR(1:20) containing 22.7 wt % of PI-05 (●). Solid line indicates a_T calculated with eq 8.

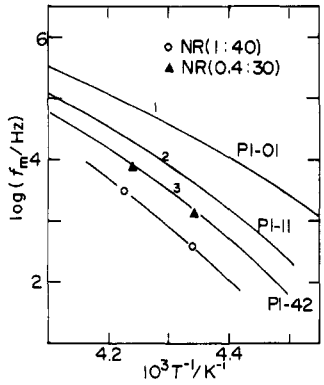

Figure 7. Arrhenius plot for the segmental-mode process for NR(1:40) and NR(0.4:30). The solid lines 1, 2, and 3 show the Arrhenius plot for PI-01, PI-11, and PI-42, respectively.

relaxation time τ_{ng} for the normal-mode process of the guest molecules in the networks, it is necessary to evaluate the difference in ζ of the networks cross-linked under various conditions.

Previously, we showed that ζ is proportional to the relaxation time τ_s for the segmental-mode process.[17] In this study, we used this relation for this purpose. First we test whether the linear relationship between τ_s and ζ holds for the networks. It is well-known that temperature dependence of τ_s is described by the Vogel equation:[16,18]

$$\log f_{ms} = A - B/(T - T_0) \quad (7)$$

where f_{ms} is the loss maximum frequency for the segmental mode equal to $1/(2\pi\tau_s)$ and A, B, and T_0 are parameters whose values for *cis*-PI were reported previously.[10] From eq 1, 5, and 7, the shift factor a_T for τ_{ng} may be written as

$$\log a_T = \log (T_r/T) + B/(T - T_0) - B/(T_r - T_0) \quad (8)$$

where T_r is the reference temperature.

Figure 6 shows an example of the T dependence of log a_T for pure NR(1:20) and NR(1:20) containing 23% PI-05. The full line represents eq 8. Since B depends little on M, we assumed that B is equal to that for PI-42 and only T_0 is an adjustable parameter. As is seen in this figure, the experimental log a_T coincides well with the shift factor calculated with eq 8, indicating that $\zeta \propto \tau_s$.

Figure 7 shows comparison of the T^{-1} dependence of log f_{ms} between the two natural rubber networks and three pure *cis*-PIs in the temperature region from 220 to 250 K. We reported previously[10] that f_{ms} for *cis*-PI of high $M > 2 \times 10^4$ is almost independent of M, but it increases with decreasing M below this molecular weight. The value of f_{ms} for NR(0.4:30) is very close to that of PI-42. The result

Table III
Relaxation Time for the Segmental Mode Process at 273 K

code	log τ_s	code	log τ_s
PI-01	-7.9	NR(0.4:40)	-7.5
PI-05	-7.7	NR(1:40)	-7.4
PI-11	-7.6	NR(1:20)	-7.4
PI-42	-7.5		

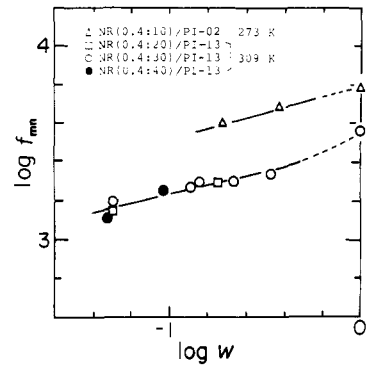

Figure 8. Double-logarithmic plot of the loss maximum frequency f_{mn} vs. weight fraction w of the guest *cis*-PI in the networks.

suggests that ζ in NR(0.4:30) is close to that in pure *cis*-PI of high M. However, the bulk-cross-linked network NR(1:40) showed lower f_{ms} than NR(0.4:30), indicating ζ is higher than that in *cis*-PI.

From the difference in τ_s around 230 K ($T^{-1} \sim 4.3 \times 10^{-3}$), we estimated the difference in τ_s at 273 K by extrapolating f_{ms} using the Vogel equation. We assumed that A and B for the networks are the same as those for PI-42 and estimated T_0 of NR(1:40) from the data of f_{ms}. By using these parameters, log τ_s at 273 K has been estimated for the networks and *cis*-PI, as listed in Table III. From this table, we see that ζ in NR(1:40) is higher than that in other samples by only 0.2 decades. Therefore, the friction coefficient is not an important factor causing the difference between the dielectric relaxation time of the entrapped and bulk *cis*-PI.

Concentration Dependence. Figure 8 shows the double-logarithmic plot of f_{mn} vs. weight fraction w of the guest for PI-13 in NR(0.4:20), NR(0.4:30), and NR(0.4:40) and for PI-02 in NR(0.4:10). We see that f_{mn} slightly increases with increasing w. Two factors may be responsible for the concentration dependence of f_{mn}: One is the change in the friction coefficient and the other is the tube renewal effect.[19]

In case of PI-13 absorbed in the networks prepared at $C_x = 0.4$, the change in f_{mn} cannot be ascribed to the change in ζ, because these networks have similar M_x to NR(0.4:30) and hence ζ in these networks is almost the same as PI-13. Since PI-13 has M slightly larger than M_c, the mobility is presumably affected by entanglement. We expect that the tube renewal effect[19] is significant in pure PI-13, but not for the guest *cis*-PI in the networks, when the guest content is low. Thus, we may attribute the concentration dependence of f_{mn} to this effect. It is noted that f_{mn} at $w = 1$ represents the value for pure PI-13 and may be quite different from f_{mn} for the network which is swollen infinitely by PI-13.

For the network containing PI-02, we can explain the change of f_{mn} as the change in ζ as described in the previous section since PI-01 having the similar molecular weight to PI-02 exhibits τ_s shorter than NR(1:40) by 0.5 decades as shown in Table III.

Molecular Weight Dependence of the Relaxation Time. Figure 9 shows the M dependence of τ_{ng} of the guest *cis*-PI absorbed in the networks at 273 K. The content

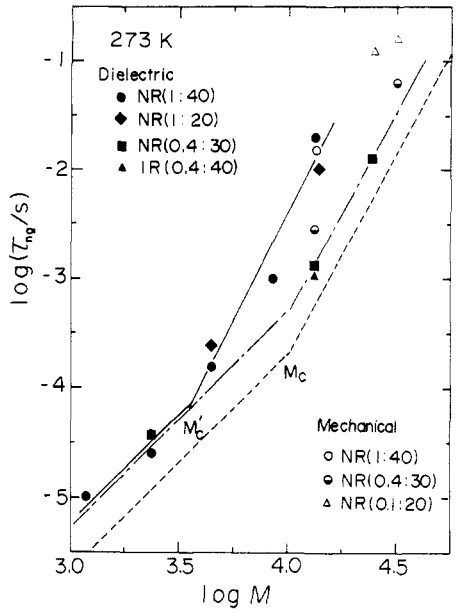

Figure 9. Molecular weight dependence of the relaxation time τ_{ng} for the normal-mode process of the guest molecules in NR(1:40), NR(1:20), NR(0.4:30), and IR(0.4:40). The solid and dash–dot lines show the estimated M dependence curve of τ_{ng} for the NR(1:40) and NR(0.4:30) systems, respectively. Dashed line represents the M dependence of the relaxation time τ_n of uncross-linked *cis*-PI. Mechanical relaxation times τ_{mg} reported in part 2 of this series are also plotted for the sake of comparison.

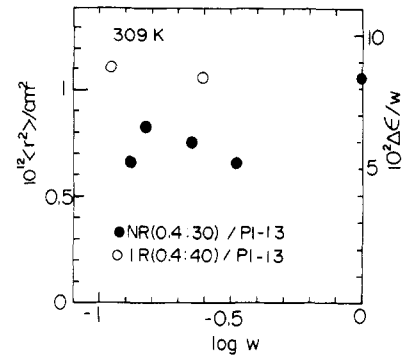

Figure 10. Mean-square end-to-end distance $\langle r^2 \rangle$ vs. weight fraction w for PI-13 absorbed in NR(0.4:30) (●) and IR(0.4:40) (○).

of the guest was controlled in the range 5–15%. For the sake of comparison, the longest mechanical relaxation time τ_{mg} for the guest *cis*-PI in the networks[2] and τ_n for pure *cis*-PI[10] were also plotted. As reported previously, the τ_ns for pure *cis*-PI show two regimes: in the range where $M < M_c$ ($\sim 10^4$), τ_n is proportional to $M^{2.0}$ in agreement with the Rouse theory, but in the range of $M > 10^4$, τ_n is proportional to $M^{3.7}$ similarly to the viscoelastic relaxation times in entangled systems.[3]

We expect that the guest molecules in NR(0.4:30) show the behavior of the regime 1 and 2 of de Gennes' phase diagram (Figure 1 of part 2), since the average value of M_{xE} and M_{xs} for this network is 5200 which is similar to M_e (=5000) of *cis*-PI. Therefore, according to the simplified view by de Gennes, the dynamic behavior of *cis*-PI in this system should be the same as that in the pure state. However, as seen in Figure 9, the τ_{ng}s for the guest molecules in NR(0.4:30) are higher than those for the corresponding pure *cis*-PI by 0.3–0.4 decades. Although data points are too sparse to draw a definite τ_{ng} vs. M curve for NR(0.4:30), we speculated it as shown by the dot–dash line in Figure 9.

The difference between τ_n and τ_{ng} at log M = 3.4 is due mostly to the change in the friction coefficient as shown in Table III. However, in the range of $M > 4.0$, the difference cannot be ascribed to the difference in ζ but presumably to the tube renewal effect[19] as described in the previous section.

As seen in Figure 9, the τ_{ng}s in NR(1:40) and NR(1:20) are longer than those in NR(0.4:30) in the range of log M > 3.6. This crossover molecular weight may be regarded as the characteristic molecular weight M'_c for this system. In linear polymers, it is known that M_c is approximately equal to $2M_e$. We compared M'_c with the average values of $2M_{xE}$ and $2M_{xs}$ which are 4300 and 4000 for NR(1:40) and NR(1:20), respectively. We see that M'_c is close to $2M_x$ as anticipated. These facts indicate that the relaxation behavior in NR(1:40) corresponds to regime 3 in de Gennes' phase diagram. The guest *cis*-PI molecules in these networks are in the strangulation state.

We note that the τ_{ng} for PI-01 and PI-02 absorbed in NR(1:40) are also longer than those of pure PI-01 and PI-02 by 0.3 decades even though these *cis*-PIs of $M < M_e$ should be in the nonentangled regime. Since the difference in τ_s and hence ζ for PI-01 is 0.3 decades (see Table III), the difference of τ_{ng} can be attributed to the difference in ζ between PI-01 and NR(1:40).

Though the plotted points are rather scattered, the slope of the log τ_{ng} vs. log M plot for the guest *cis*-PI in NR(1:40) is determined to be 4.0 ± 0.5. It seems that this plot is not a straight line but an upward concave curve with the slope becoming steeper with increasing M. This behavior is quite different from that predicted by the tube model.

Next, we compare τ_{ng} with the mechanical relaxation time τ_{mg} of guest *cis*-PIs in the networks reported in part 2 of this series.[2] As shown in Figure 9, the τ_{ng} and τ_{mg} in NR(1:40) coincide well, but the τ_{mg} in NR(0.4:30) are slightly longer than the τ_{ng}. Since the experimental error in mechanical data was relatively high,[2] we may conclude that the τ_{mg} coincides roughly with the τ_{ng}, irrespective of the strangulation effect.

Here we comment briefly on the relationship between τ_{ng} and τ_{mg}. The Zimm[14] theory predicted $\tau_{ng} = 2\tau_{mg}$ for nonentangled chains. Previously, we confirmed that this relation is valid for cis-PI with $M < M_c$ by comparing τ_n with τ_m calculated with eq 3 from a zero-shear viscosity reported by Nemoto et al.[20] However, in the entangled region, the tube theory[6,7] predicts that $\tau_{ng} = \tau_{mg}$. The result shown in Figure 9 indicates that this τ_{ng} in the entangled region appears to be equal to τ_{mg}, in agreement with the tube model.

Dielectric Relaxation Strength. From the dielectric relaxation strength $\Delta\epsilon$ for the normal mode process, we can determine $\langle r^2 \rangle$ using eq 2. The relaxation strength was determined from the area surrounded by the ϵ'' curves for the networks with and without the guest *cis*-PI. Figure 10 shows the values of $\langle r^2 \rangle$ for PI-13 absorbed in NR(0.4:30) and RI(0.4:40). As is seen in this figure, $\langle r^2 \rangle$ in the natural rubber network is smaller than that in pure *cis*-PI or that in a Θ solvent.

One of the reasons for this behavior may be due to the difference in the microstructures between natural rubber and anionically polymerized high *cis*-PI: the former has almost 100% cis structure, but the latter only 80% cis. Usually, interaction between two polymers differing in the chemical structure is repulsive. Therefore, a weak repulsive force between the *cis*-PI and natural rubber might cause the decrease in the dimension below the unperturbed dimension.

This is supported by the value of $\langle r^2 \rangle$ for *cis*-PI in IR(0.4:40), the microstructure of which is the same. As shown

in Figure 10, the end-to-end distance of *cis*-PI in this system is close to the value in pure PI-13. Therefore, the smaller relaxation strength for *cis*-PI in the natural rubber network rather than that in the *cis*-PI network is due to the repulsive interactions between NR and *cis*-PI.

Conclusions

Due to relatively large experimental error involved and the limitation of the range of the sample molecular weight covered in this study, we cannot draw definite conclusions in the present stage. However, the following qualitative conclusions can be drawn:

1. The relaxation time τ_{ng} for the normal-mode process of the guest *cis*-polyisoprene in cross-linked natural rubber is longer than that in the undiluted *cis*-polyisoprene.
2. When M_x is lower than M_e, τ_{ng} becomes longer than that of the corresponding *cis*-PI. This result may be attributed to the strangulation effect.
3. The relaxation strength for the guest *cis*-PI in cross-linked natural rubber is smaller than that in pure *cis*-PI. This indicates that the mean-square end-to-end distance is smaller than the unperturbed dimension. However, $\Delta\epsilon$ for the guest *cis*-PI in the network prepared from a synthetic *cis*-PI sample is almost the same as the *cis*-PI in the bulk state.

Acknowledgment. B. T. Poh thanks the Japan Society of Promotion of Science for granting a fellowship to him to carry out this work. This work was supported in part by the Grant-in Aid for Scientific Research (60470107 and 6055062) by the Ministry of Education, Science and Culture, Japan. Support from the Institute of Polymer Research, Osaka University, is also acknowledged.

Registry No. Polyisoprene, 9003-31-0.

References and Notes

(1) Poh, B. T.; Adachi, K.; Kotaka, T. *Macromolecules*, second preceding paper in this issue.
(2) Poh, B. T.; Adachi, K.; Kotaka, T. *Macromolecules*, preceding paper in this issue.
(3) de Gennes, P.-G. *Macromolecules* **1986**, *19*, 1245.
(4) Ferry, J. D. *Viscoelastic Properties of Polymers*, 3rd ed.; Wiley: New York, 1980.
(5) Rouse, P. E. *J. Chem. Phys.* **1953**, *21*, 1272.
(6) de Gennes, P.-G. *J. Chem. Phys.* **1971**, *55*, 572.
(7) Doi, M.; Edwards, S. F. *J. Chem. Soc., Faraday Trans. 2* **1978**, *74*, 1789.
(8) See references cited in the preceding paper (part 2).
(9) Adachi, K.; Kotaka, T. *Macromolecules* **1984**, *17*, 120.
(10) Adachi, K.; Kotaka, T. *Macromolecules* **1985**, *18*, 466.
(11) Adachi, K.; Okazaki, H.; Kotaka, T. *Macromolecules* **1985**, *18*, 1687.
(12) Adachi, K.; Kotaka, T. *Macromolecules*, in press.
(13) Adachi, K.; Okazaki, H.; Kotaka, T. *Macromolecules* **1985**, *18*, 1486.
(14) Zimm, B. H. *J. Chem. Phys.* **1956**, *24*, 269.
(15) Shy, L. Y.; Eichinger, B. E. *Macromolecules* **1986**, *19*, 2787.
(16) Berry, G. C.; Fox, T. G. *Adv. Polym. Sci.* **1968**, *5*, 261.
(17) Adachi, K.; Kotaka, T. *Nihon Reoroji Gakkaishi* **1986**, *14*, 99.
(18) Vogel, H. *Z. Phys.* **1921**, *22*, 645.
(19) Klein, J. *Macromolecules* **1978**, *11*, 852.
(20) Nemoto, N.; Odani, H.; Kurata, M. *Macromolecules* **1972**, *5*, 531.

Transient Electric Birefringence Measurements of the Rotational and Internal Motions of a 1010 Base Pair DNA Fragment—Field Strength and Pulse Length Effects

Roger J. Lewis[†] and R. Pecora*

Department of Chemistry, Stanford University, Stanford, California 94305

Don Eden

Department of Chemistry, San Francisco State University, San Francisco, California 94132.
Received October 4, 1986

ABSTRACT: We examine the effects of the electric field strength and the orienting pulse duration on the measured decay of the transient electric birefringence of a blunt-ended DNA restriction fragment 1010 base pairs in length (molecular weight 670 000) in solution. Effects of pulse length on the distribution of decay times which were shown in an earlier work (Lewis, R. J.; Pecora, R.; Eden, D. *Macromolecules* **1986**, *19*, 134) are examined in greater detail, allowing us to determine the approximate time course for the excitation of each of the first three decay modes. The rise times of the first two modes are very similar, but the decay times are quite different. Two qualitative approaches are presented to explain the excitation time courses of the various modes. The first emphasizes the motion of different populations of counterions while the second postulates the exchange of excitation between different modes. In addition, by increasing the applied field strength, we observe a decrease in the average birefringence decay time before there is deviation from a modified form of the Kerr law. A similar decrease in the average decay time has been observed by Diekmann et al. (Diekmann, S.; Hillen, W.; Morgeneyer, B.; Wells, R. D.; Porschke, D. *Biophys. Chem.* **1982**, *15*, 263) and Stellwagen (Stellwagen, N. C. *Biopolymers* **1981**, *20*, 399).

Introduction

In previous work[1] we demonstrated that the zero-field electric birefringence decay from each of four monodisperse DNA fragments in solution could be resolved into several distinct exponential decays. We designated the slowest of these decay modes the "rotational decay mode" even though, in flexible DNAs, it probably represents a coupled bending-rotational motion. We attributed the faster decay modes to internal bending motions in the DNA fragments, although the possibility exists that these faster modes may contain a significant rotational component. The predictions of two dynamic models, the "trumbell" model of Roitman and Zimm[2-4] and the Rouse–Zimm model of Zimm,[5,6] compared favorably with the experimental results. The reader is referred to the earlier work[1,7] for additional details. Contrary to a statement in our earlier work[1] the

[†]Present address: Department of Emergency Medicine, Los Angeles County—Harbor—UCLA Medical Center, 1000 West Carson Street, Torrance, CA 90509.

0024-9297/87/2220-2579$01.50/0